Design and control of acetonitrile/ N -propanol separation system via extractive distillation using N -methyl pyrrolidone as entrainer

Article *in* Separation Science and Technology · March 2018

DOI: 10.1080/01496395.2018.1450425

CITATIONS
12

READS
259

6 authors, including:

Weiyi Su
Hebei University of Technology
47 PUBLICATIONS **594** CITATIONS

SEE PROFILE

Separation Science and Technology

ISSN: 0149-6395 (Print) 1520-5754 (Online) Journal homepage: http://www.tandfonline.com/loi/lsst20

Design and control of acetonitrile/N-propanol separation system via extractive distillation using N-methyl pyrrolidone as entrainer

Honghai Wang, Lulu Xue, Weiyi Su, Xu Li, Yue Li & Chunli Li

To cite this article: Honghai Wang, Lulu Xue, Weiyi Su, Xu Li, Yue Li & Chunli Li (2018): Design and control of acetonitrile/N-propanol separation system via extractive distillation using N-methyl pyrrolidone as entrainer, Separation Science and Technology, DOI: 10.1080/01496395.2018.1450425

To link to this article: https://doi.org/10.1080/01496395.2018.1450425

Published online: 20 Mar 2018.

SEPARATION SCIENCE AND TECHNOLOGY
https://doi.org/10.1080/01496395.2018.1450425

Taylor & Francis
Taylor & Francis Group

Design and control of acetonitrile/*N*-propanol separation system via extractive distillation using *N*-methyl pyrrolidone as entrainer

Honghai Wang, Lulu Xue, Weiyi Su, Xu Li, Yue Li, and Chunli Li

School of Chemical Engineering & Technology, Hebei University of Technology, Tianjin, China

ABSTRACT

The extractive distillation process for separating a binary azeotrope of acetonitrile and *n*-propanol is investigated using *N*-methyl pyrrolidone as entrainer. On the basis of multiparameter optimization, a design with optimized operation conditions for the process is presented. Two dynamic control structures are proposed. Feed disturbances are used to evaluate the dynamic performance. The response results reveal that the control structure CS1 with temperature–composition cascade control loop can handle all the disturbances and maintain product purities, except one large transient deviation, while the improved control structure CS2 with average temperature control loop can overcome this obstacle and handle disturbances effectively.

ARTICLE HISTORY
Received 25 October 2017
Accepted 6 March 2018

KEYWORDS
Extractive distillation; optimization; control structure; dynamic simulation

Introduction

Acetonitrile and *n*-propanol are widely applied in chemical industries which can be used as mobile phase in liquid chromatography and electrolytes in electrochemistry.[1,2] The acetonitrile and *n*-propanol mixture are common in industry, such as mixture of acetonitrile *n*-propanol and water in fine chemical industry, which may cause environmental pollution if discharged directly.[3] Therefore, the separation and recycle of these two chemicals are necessary. Typically, distillation is accepted as an efficient method for separating and purifying the mixture.

Since acetonitrile and *n*-propanol form a minimum boiling azeotrope at atmospheric pressure, several alternative distillation methods have been introduced including extractive distillation,[4,5] pressure swing distillation[6,7] and so on. For extractive distillation, a suitable entrainer is usually introduced to enhance the relative volatility between the binary azeotrope. He[8] used extractive distillation with salt to separate acetonitrile/*n*-propanol mixture. Although it showed a good efficiency of separation, the recovery of salt was much difficult. Additionally, Fang[9] used ionic liquid as entrainer; although the separation results were reasonable, the price of ionic liquids is expensive. In order to select an economical and effective solvent, Zhao[10] used UNIFAC group contribution method[11] and found that *N*-methyl pyrrolidone (NMP) showed the best effect.

As to extractive distillation process optimization,-[12,13] many operating parameters, such as feed, reflux ratio, solvent,[14] should be considered. In order to deal with the interaction among parameters, Wang[15] introduced the statistical analysis method, orthogonal design and response surface methodology and the results were in accordance with experiment data tightly.

Furthermore, dynamic control is necessary due to the flow rate and component disturbances. Accordingly, the dynamic control of distillation system can be implemented in Aspen dynamic. Luyben[6,16–18] have done significant work and provided fundamental guidance for distillation control. Many effective control strategies showed good dynamic responses to various fluctuations.[19,20] However, control strategies varied with distillation systems. For instance, Rafiqul[21] explored and estimated the use of variable measurement and found that various operating conditions cause variations in resulting control schemes. Kai-Yi Hsu[22] proposed a simple overall control structure for distillation process in which one tray temperature control loop was applied and the products purities were maintained despite feed disturbances. Similarly, Saiful[23] proposed a temperature-component control structure in an extractive distillation, and the results revealed that fixing reflux ratio contributes to reducing feed disturbances. Additionally, a reflux-to-feed ratio scheme with a composition controller was applied to address feed flow fluctuations according to Bao.[24] Moreover, Yang[19] presented a dual-end temperature control structure and could deal with feed disturbances effectively. However, the design and control analysis on separation of acetonitrile/*n*-propanol mixture

CONTACT Prof. Chunli Li lichunli_hebut@126.com School of Chemical Engineering, Hebei University of Technology, Tianjin 300130, China.
Color versions of one or more of the figures in the article can be found online at www.tandfonline.com/lsst.

was limited. So, it is desirable to explore an optimized design and feasible control structure for this mixture with emphasis on purifying the products and stabilizing the process.

In this paper, an extractive distillation is performed to separate binary azeotrope of acetonitrile and *n*-propanol, while NMP is selected as a suitable entrianer. Then, a better combination of operating conditions is selected on the basis of multiparameter analysis to reduce energy consumption and enhance products purities. To prevent the strong interaction among parameters, effective dynamic control structures are designed. The results of simulation and control structure will provide fundamental guide for the industrialization design and production.

Steady state design

Entrainer selection

Since entrainer is a dominant factor in the feasibility of the extractive distillation, efforts should be paid to selection. The relative volatility is a criterion for entrainer selection. The higher the relative volatility, easier the separation will be. Four entrainer candidates feasible for the separation of acetonitrile and *n*-propanol azeotrope mixture are studied in this work: glycerol, dimethylformamide, dimethyl sulfoxide and NMP. The bubble points (T_b) and the relative volatility are listed in Table 1.[25] NMP shows a higher relative volatility and doesn't introduce other azeotropes to the system; so, it is chosen as the entrainer.

Thermodynamic model and feasibility analysis

An appropriate thermodynamic model can predict and provide accurate data for the process simulation. In this case, part of the binary interaction parameters was regressed with the experimental data,[26] while the missing part was predicted by the activity coefficient model, UNIFAC,[25] a group contribution-based method, in Aspen Plus.

Residue curve map (RCM) is considered as powerful tool for flowsheet design, conceptual design and feasible sequence within a given system. The RCM of acetonitrile–*n*-propanol–NMP ternary system mapped with Aspen Plus is shown in Fig. 1.

Table 1. Results of the entrainer selection for extractive distillation system.

Entrainer	Molecular formula	T_b (°C)	Relative volatility
Glycerol	$C_3H_8O_3$	290	1.315
DMF	C_3H_7ON	153	1.275
DMSO	C_2H_6OS	189	1.555
NMP	C_5H_9ON	204	2.176

It is observed that acetonitrile/*n*-propanol azeotrope is unstable node, NMP is the stable node, acetonitrile and *n*-propanol are the saddles. The resulting residue curves (golden lines) with arrows point to pure NMP. It demonstrates no distillation boundary exists and an ideal extractive distillation situation. The red line is the univolatility curve and useful for conceptual design. Usually, smaller truncation point (X_E) means smaller amount of entrainer and lower investment. The blue lines are material balance lines. It is noticed that F1 is separated into D1 and B1, and B1 is separated into D2 and B2. This means the azeotrope mixture can be separated into relatively pure products with the help of the entrainer. Besides, a small makeup of NMP should be added to balance the entrainer loss.

Flowsheet

The process for the acetonitrile/*n*-propanol separation using NMP as the entrainer is shown in Fig. 2. It consists of an extractive distillation column (EDC) and an entrainer recovery column (ERC). The fresh feed mixture is fed to lower portion and the pure entrainer to upper portion of EDC. Theoretically, the entrainer alters the relative volatility of the azeotropic mixture, thus acetonitrile (light component) can be gathered in the distillate (D1) and the mixture of *n*-propanol (heavy component) and NMP enriches at the bottom (B1). Then, B1 is fed to the ERC to get *n*-propanol product in the distillate (D2) and almost pure NMP in the bottom (B2). NMP recycles back to the

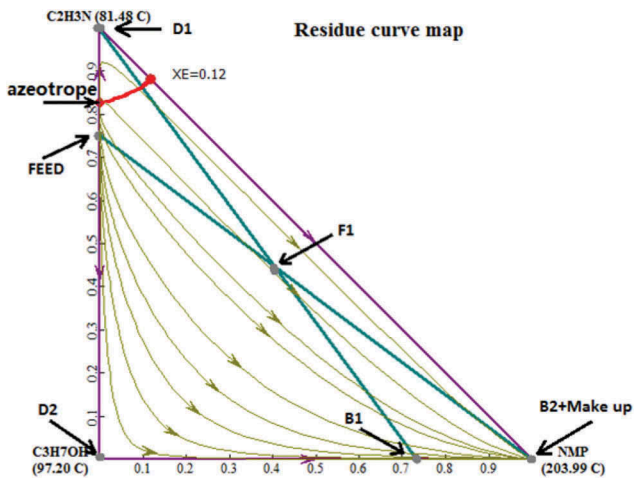

Figure 1. Residue curve map at 1 atm for acetonitrile/*n*-propanol/NMP system.

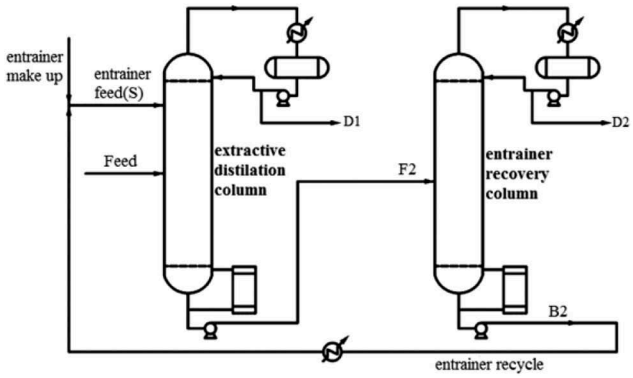

Figure 2. The flowsheet of extractive distillation simulation.

EDC, and a small make up of NMP is needed to balance the minor loss.

Multiparameter optimization analysis

The steady-state simulation was performed in Aspen Plus V7.2. The process flow sheet for the system was designed and shown in Fig. 2. The trays in columns are numbered from top to the bottom. To establish the operating conditions for the extractive distillation process, various parameters need to be optimized. Because this process is based on an actual industrial process, operation conditions should get very close to the real process: feed flow rate (F = 1000 kg/h), feed composition (75 wt% acetonitrile and 25 wt% *n*-propanol), feed temperature (T_{F1} = 25°C), operating pressure (1 atm), distillate rate of two columns (D1 = 750 kg/h, D2 = 250 kg/h). The analyzed parameters are as follows: the reflux ratios (R1 and R2), the feed stages (N_{F1} and N_{F2}), the entrainer feed stage (N_S) and temperature (T_S), entrainer to feed ratio (S/F). The two product purities are required over 99.8 wt %. The object functions are the heat duty of reboilers (Q_{reb1} and Q_{reb2}) and product purity (X_{D1} and X_{D2}). The extractive distillation is a nonlinear process; there are interactions among the operating parameters, which may have different effects on objective functions. Therefore, all the associated parameters should be considered and a multiparameter optimization analysis is carried out with the assistance of the response surface method[15] and the Aspen fixed function sensitivity analysis.

Effects of entrainer-to-feed ratio (S/F) and reflux ratio (R1) on EDC

Fig. 3 shows the influences of entrainer ratio (S/F) and reflux ratio (R1) on reboiler duty (Q_{reb1}) and product mass purity (X_{D1}). It is shown in Fig. 3(a) that the energy consumption increases when R1 or S/F is added, and R1 affects more on Q_{reb1} compare to S/F. For a preset extractive distillation process, S/F ratio and reflux ratio must reach a certain value to achieve separation objective. However, the higher the S/F ratio or reflux ratio is, the more energy consumption will be so that the minimum S/F ratio must be determined to meet product purity and the accurate S/F ratio is selected based on controllability and lower energy consumption.

It is noticed in Fig. 3(b) that the influence of R1 on product purity is not monotonous for a fixed S/F ratio. The acetonitrile purity can reach the maximum when R1 get larger; however, the overfull reflux ratio may bring adverse effect. That because more entrainer collects at column top if reflux flow is small. And that causes product concentration reduction. However, the surplus acetonitrile (light component) dilutes the concentration of NMP if reflux flow is large. So, the actual entrainer proportion is declined, the relative volatility of the azeotrope mixture declined; subsequently, it offsets the contribution of reflux ratio and more *n*-propanol (heavy component) go to the top. On the other hand, it is known that entrainer influences product purity greatly; in Fig. 3, we can find that the acetonitrile purity increases when the S/F ratio is larger for a fixed

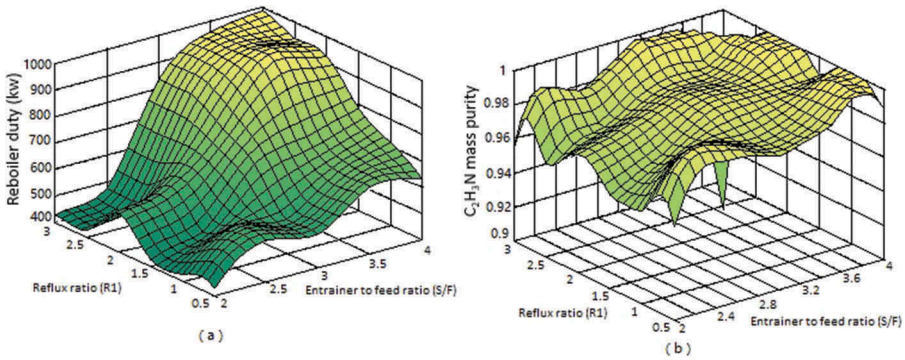

Figure 3. Effects of entrainer ratio and reflux ratio on reboiler duty and C_2H_3N purity of EDC.

reflux ratio. As a result, R1 is determined to be 1–2 and the minimum S/F ratio is 2.5–3.

Effects of feed stage and entrainer feed stage on EDC

Fig. 4 shows the effects of feed stage (N_{F1}) and entrainer feed stage (N_S) on reflux ratio (R1) and reboiler duty (Q_{reb1}), meanwhile maintaining the product purity. It is noticed in Fig. 4(b) that N_S has little influence on reboiler duty when N_{F1} is more than 16. And, the minimum Q_{reb1} occurs when N_{F1} is between 14 and 16, N_S is between 4 and 5. Correspondingly, the minimum reflux ratio is between 1 and 1.5 in Fig. 4(a). It is reasonable that the rectifying section enlargement contributes to purity of light component in distillate; however, there must be a suitable distance between N_{F1} and N_S to accomplish azeotrope separation target. Moreover, the rectifying section must ensure enough space to avoid NMP distillated from the top and resulting in entrainer loss.

Effects of reflux ratio and entrainer feed temperature on EDC

The effect of reflux ratio (R1) and entrainer feed temperature (T_S) on reboiler duty (Q_{reb1}) of EDC and product purity are shown in Fig. 5. It is obvious that Q_{reb1} increases as R1 is added with a fixed T_S. And, the Q_{reb1} decreases as T_S is added with a fixed R1. And, the reboiler duty changes slowly when T_S changes so that the optimal R1 is 1.4–2, and T_S is 95–100°C.

Effects of stage number (N1) and entrainer to feed ratio (S/F) on EDC

The stage number is an important factor in extractive distillation process. If the number is small, it can not reach the separation target. On the other hand, the large number of stages may cause equipment waste. Fig. 6 shows the effects of stage number (N1) and entrainer to feed ratio (S/F) on the product purity and reboiler duty (Q_{reb1}). With the increase of stage number, the purity of acetonitrile increases obviously, while the reboiler duty has small change. So, the optimal N1 is 30–33.

Effects of stage number (N2) and reflux ratio on ERC

Fig. 7 shows the effects of stage number (N2) and reflux ratio on the product purity and reboiler duty (Q_{reb2}). When the stage number increases, the purity of *n*-propanol increases slowly and reboiler duty changes slowly, which indicates the good ability of separation. So, the optimal N2 is 12–16.

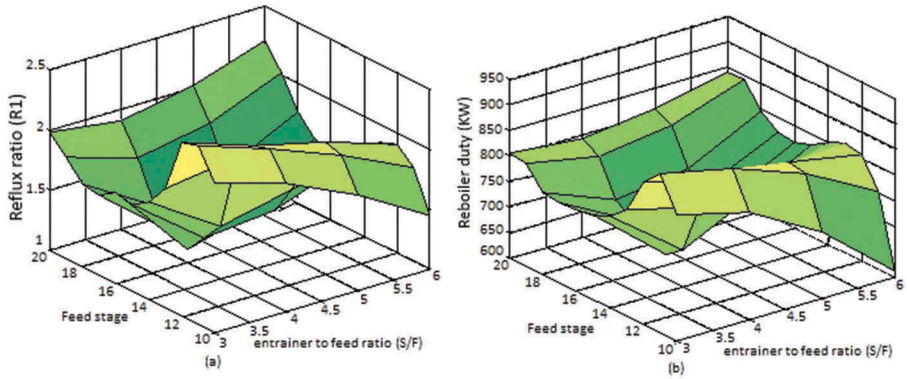

Figure 4. Effects of feed stage and entrainer feed stage on reflux ratio and reboiler duty of EDC.

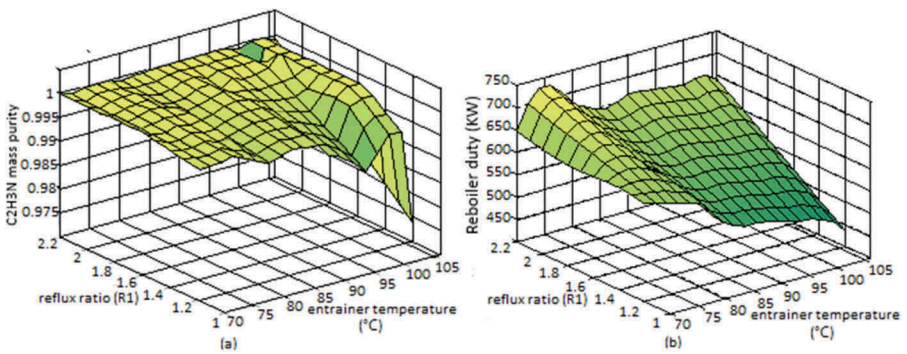

Figure 5. Effects of reflux ratio and entrainer temperature on C_2H_3N purity and reboiler duty of EDC.

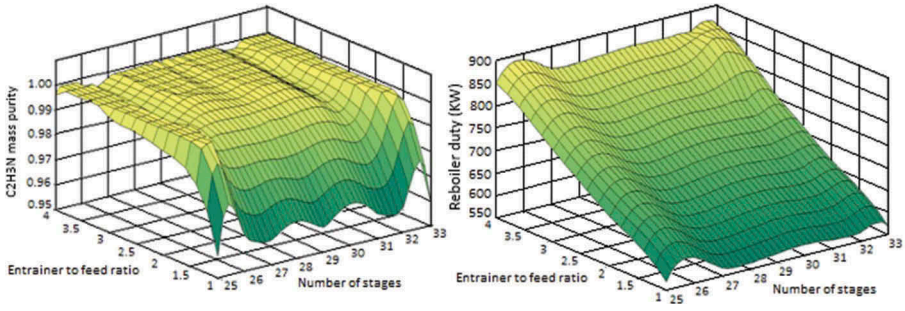

Figure 6. Effects of stage number (N1) and entrainer to feed ratio (S/F) on EDC.

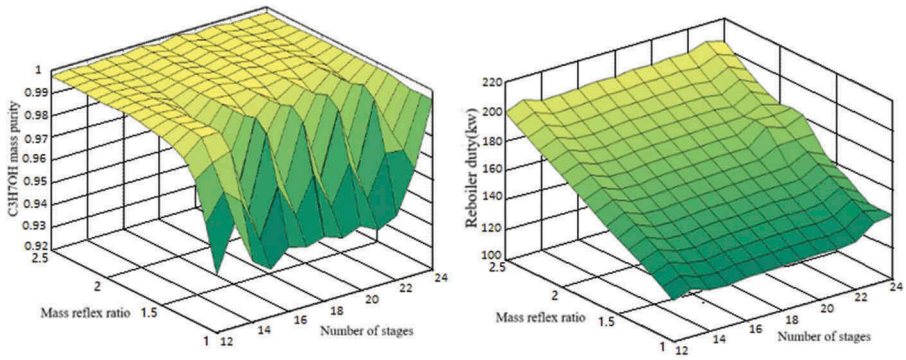

Figure 7. Effects of stage number (N2) and reflux ratio on ERC.

Effects of reflux ratio and feed stage on ERC

The effect of the reflux ratio (R2) and mixture feed stage (N_{F2}) on EDC reboiler duty (Q_{reb2}) is shown in Fig. 8 while ensuring the product purity. It shows that Q_{reb2} increases when R2 is added, and N_{F2} almost does not affect the reboiler duty. More importantly, R2 influences the controllability of ERC. The ERC is more controllable as R2 increases appropriately, which contribute to offset the energy consumption. The optimal N_{F2} is from 5 to 8 and R2 is between 1.3 and 1.8.

The optimal steady-state design is shown in Fig. 9. In EDC, the feed stage is 15 and entrainer feed stage is 4, the reflux ratio is 1.4, the S/F ratio is 3 and entrainer temperature is 95°C. In ERC, the feed stage is 6, the reflux ratio is 1.4. The purity of acetonitrile is 0.9981 and *n*-propanol is 0.9983, Q_{reb1} is 584 kW and Q_{reb2} is 147 kW.

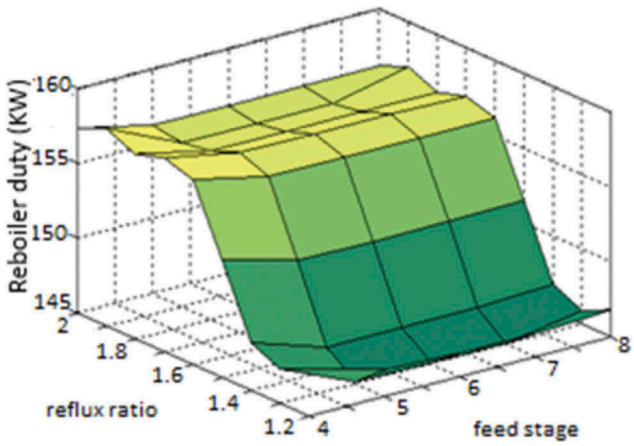

Figure 8. Effect of reflux ratio and feed stage on reboiler duty of ERC.

Dynamic control of extractive distillation system

Conversion from steady-state to dynamic simulation

The calculated sizes of the equipment are specified in the steady-state simulation before dynamic simulation via the commonly used heuristicas.[22] According to this method, there must be 5–10 min of liquid holdup when vessels are half full, based on the liquid content entering or leaving the vessel. For reflux drum, the holdup is sum of the liquid distillate and the reflux. For column base, it is the liquid entering the reboiler from the bottom tray. The pressure drops of the control valves are specified as 3 bar with half open of the valves. Then, pressure of the steady state simulation is checked and exported to the pressure driven dynamic simulation.

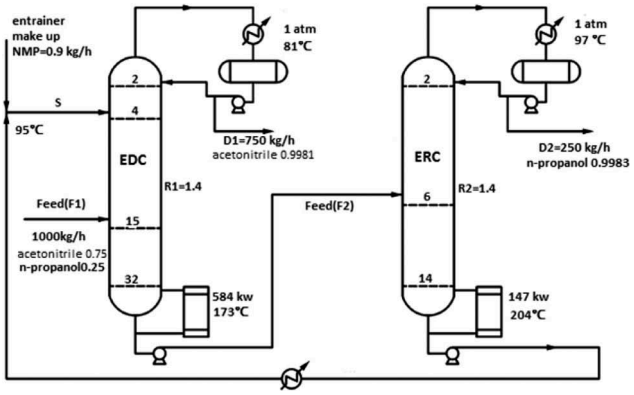

Figure 9. The steady-state process flowsheet of extractive distillation.

Sensitivity analyses of tray temperature

Temperature is usually used as an indicator of product purity in distillation control due to the obvious change of the temperature difference from tray to tray. The temperature distribution profile of EDC and ERC is shown in Fig. 10. As can be seen in Fig. 10(a), the temperature distribution is irregular. Stage 4, 22, and 31 show sharp changes. Specifically, the temperature on stage 4 and 31 changes greatly because of the feed stream and installation of reboiler, respectively, so it can't be chosen. However, in Fig. 10(b), stage 4 shows the maximum temperature difference. As result, stage 22 and 4 are chosen as the temperature sensitive stage in each case.

Control structure (CS1)

The control structure CS1 with temperature and composition cascade for the extractive distillation process is shown in Fig. 11. The following controllers are added to the control structure:

(1) Feed is controlled by the flow rate (reverse acting).
(2) The entrainer flow is cascade control. Entrainer-to-feed ratio is 3 (reverse acting).
(3) The column pressure is controlled by manipulating heat removal rate in condenser (reverse acting).
(4) The reflux drum level is held constant by manipulating distillate rate (direct acting).
(5) The base level of EDC is maintained by adjusting bottom flow rate. The base level of ERC is held constant by manipulating entrainer make-up flow rate (reverse acting).

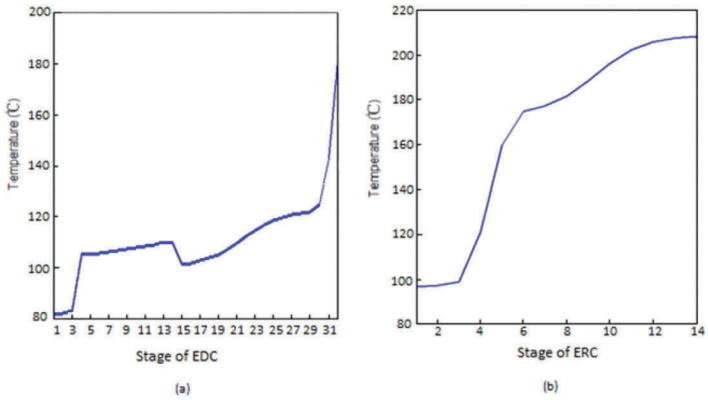

Figure 10. Temperature distribution profile of EDC and ERC.

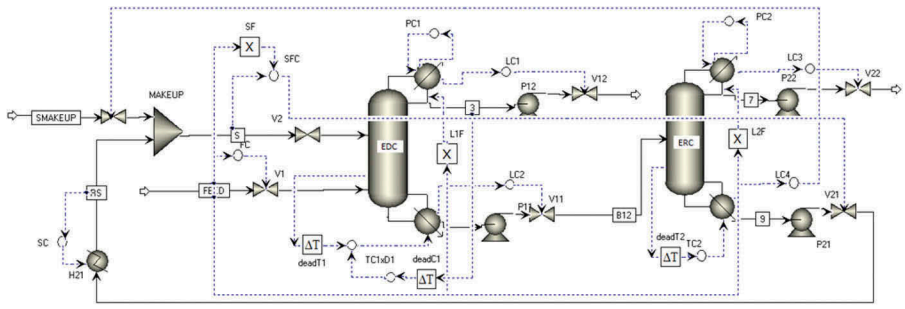

Figure 11. Diagram of control structure CS1.

(6) The tray temperature is maintained by adjusting the reboiler duty (reverse acting).
(7) The reflux flow rate and feed flow rate is proportionally controlled (reverse acting).
(8) The entrainer temperature is controlled by manipulating the heat removal rate of condenser (reverse acting).

Traditional proportional and integral (PI) controllers are employed for the whole system except the level controllers. The PI settings of the flow control and the pressure control loops are K_c = 0.5, τ = 0.3 min, and K_c = 20, τ = 12 min, respectively. In addition, proportional controllers with K_c = 2 are utilized for level controllers. Three dead time elements are used in the temperature–composition control loops. Specifically, the dead time in the temperature and composition control loop is set as 3 and 5 min, respectively. Relay feedback tests and Tyreus Luyben turning are utilized to calculate the ultimate gains and integral time of these controllers. The tuning parameters of temperature–composition controllers in CS1 are listed in Table 2. It shows that composition–temperature cascade controllers have bigger gain and shorter integral time compared to simple temperature controllers.

Table 2. The controllers tuning parameters.

Parameters	Controlled variable	Manipulated variable	Gain K_c	Integral time τ (min)
TC1	X_{D1}, T22	Q_{reb1}	2.97	9.24
TC1 × D1	X_{D1}, T22	Q_{reb1}	5.35	5.08
TC2	X_{D2}, T4	Q_{reb2}	1.57	13.2
TC2ave	X_{D2},Taverage	Q_{reb2}	3.22	7.24
FC	Feed flow	V1	0.5	0.3
SFC	Extractive solvent flow	V21	0.5	0.3
LC1–LC4	D1, 2, B1, SMAKEUP	V12,22,11 VS	2	999
PC1–2	P1, 2	$Q_{con1,2}$	20	12

The disturbances of the feed flow rate and composition are introduced to test the dynamic performance of the basic control structure CS1.

The dynamic responses of operating parameters to feed flow rate disturbance are shown in Fig. 12 for CS1. In Fig. 10(a), when 20% step change of feed flow rate takes place, the flow rate of all streams is effectively controlled and reaches stable states eventually. However, the response of the ERC distillate rate (D2) is not ideal compare to other streams; its response time

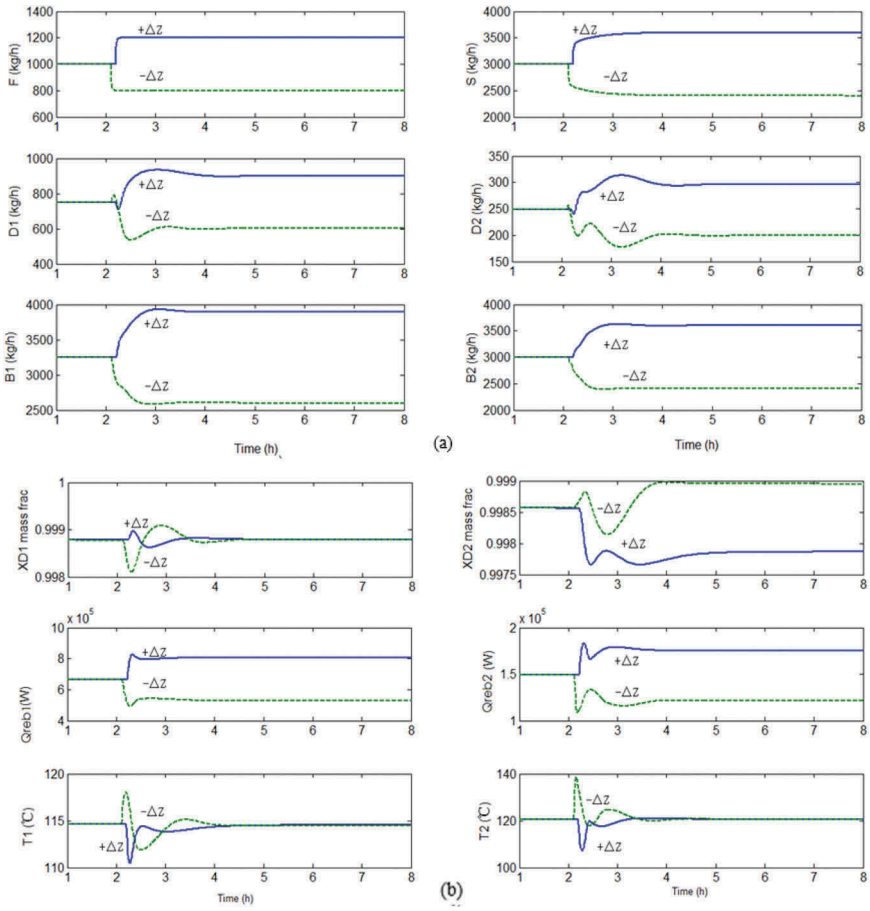

Figure 12. CS1 dynamic response curve of variables in feed flow ±20% disturbance.

is longer and has obvious wave. The product purity also has sensitive response to the disturbance: acetonitrile purity (X_{D1}) in EDC turns back to the desired value after 2 h and the maximum deviation is less than 0.1wt %, while *n*-propanol purity (X_{D2}) in ERC reaches another stable level after 2 h. Additionally, the sensitive tray temperature (T1) in EDC has a small deviation less than 5°C, but the sensitive tray temperature (T2) in ERC has a step change of 20°C, which clearly reflects the wave of *n*-propanol purity with the disturbance, which proves the rule temperature is an indicator of composition. Therefore, this phenomenon demonstrates that control structure CS1 could achieve a stable control in terms of the products purity, but it can only handle the control of acetonitrile purity (X_{D1}) in EDC effectively, but not the *n*-propanol purity (X_{D2}) in ERC.

Fig. 13 shows the dynamic responses of operating parameters to the feed composition disturbance at t = 2 h for the control structure CS1. As shown in Fig. 13(a), when the content of acetonitrile in the feed flow increases from 75% to 80 wt%, the distillate rate of EDC increases, the bottom rate of EDC and ERC both decrease and the proportion of *n*-propanol in B2 decreases as well. Meanwhile, the bottom rate of ERC returns to the initial state with a maximum range of 20 kg/h. Luckily, all flows come to a new stable level after 1 h. As we all know, during distillation, process light and heavy components gather at top and bottom of column, respectively. With the increase of acetonitrile (light component), less *n*-propanol (heavy component) gathers at bottom; therefore, the EDC reboiler duty (Q_{reb1}) decreases about 0.2×10^5 W and the sensitive tray temperature (T1) of EDC decreases. Meanwhile, more acetonitrile gathers at the top and the reflux drum level increases. And, the reflux remains unchanged for which there is a reflux and feed flow rate proportion controller (L1/F); consequently, the distillation rate (D1) increases. Correspondingly, the performances of ERC change as follows: the flow rate and component of *n*-propanol decrease, the duty of reboiler (Q_{reb2}) decreases about 0.2×10^5 W; however, sensitive tray temperature (T2) has an overshoot within 5°C. As to products purity, the purity of acetonitrile (X_{D1}) turns back to the desired value rapidly and the maximum

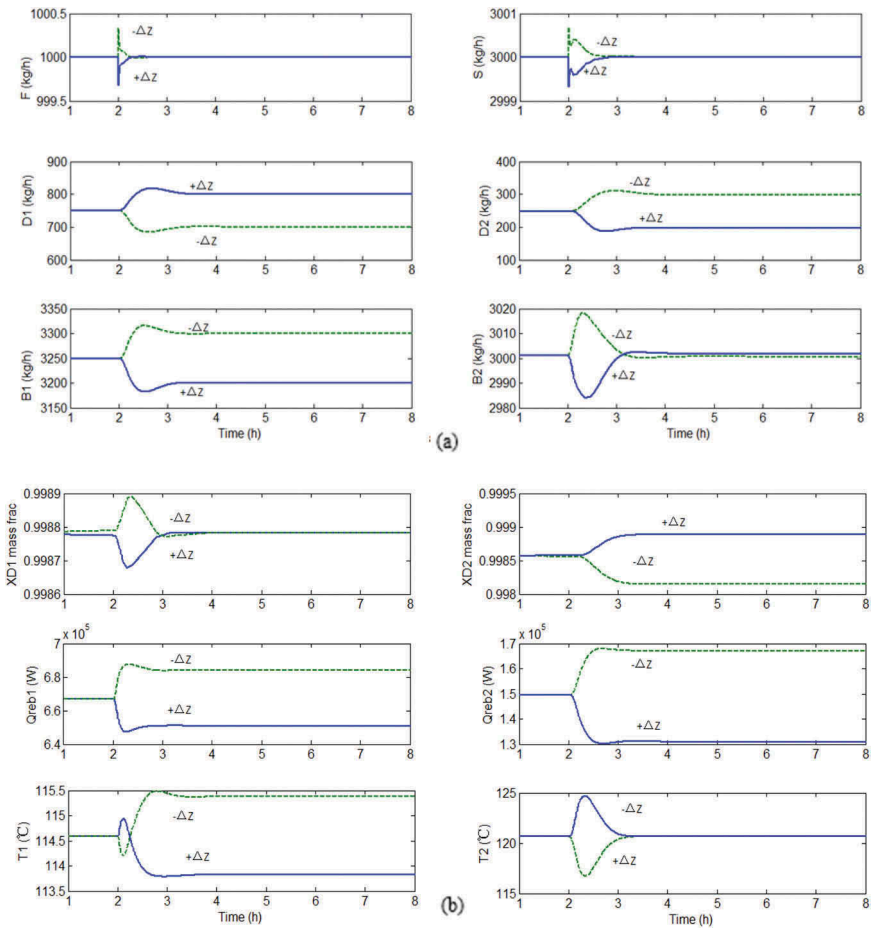

Figure 13. CS1 dynamic response curve for the feed composition of acetonitrile ±5%.

deviation is less than 0.1 wt%, while the purity of *n*-propanol (X_{D2}) reaches a stable level with reasonable deviation after 1 h.

Improved control structure CS2

An average temperature control loop is introduced in the ERC in the control structure CS2, since the sharp temperature profile in Fig. 10(b) would produce a very large process gain. The temperatures on three trays are measured: stage 3 at 98°C, stage 4 at 121°C and stage 5 at 158°C. The Multi-Sum controller and Multiply controller are installed to realize the average temperature control (TC2ave). Relay feedback tests are run and Tyreus–Luyben turning is utilized to calculate ultimate gains and integral time of these controllers. The results are listed in Table 2; the gain is higher and the integral time is smaller than that of CS1, which means a tighter control with the average temperature control structure.

Additionally, a dynamic lag is inserted to the R1/F and R2/F ratio loop in Fig. 14; the feed flow rate signal passes through a first-order lag of 5 min so that the change in reflux does not occur instantaneously with feed flow rate change. The reason should probably be that this provides dynamic compensation in the "feed forward" ratio loop; so, the response of feed flow change can match reflux change response at once, which delays the reflux rate signal, and subsequently can avoid the dynamic timing problem so that the average temperature control loop in ERC can resist disturbances effectively.

The same disturbances are used to assess the dynamic performance of control structure CS2. Figs. 15 and 16 show the dynamic responses to the feed flow rate and composition disturbances.

When 20% step feed flow rate change introduced, it can be seen from Fig. 15(a) that the EDC and ERC distillate rates (D1 and D2) have little wave and soon achieve stable state which indicates a better dynamic response than that of CS1. Additionally, in Fig. 15(b), the ERC sensitive trays temperature (T2) is obtained with transient settling out in about 1 h and T2 has a very small overshoot of 5°C. Meanwhile, the purity of *n*-propanol in ERC (X_{D2}) maintains a high level and meet the required purity (99.8%) all the time, which is much better than CS1. Obviously, the average temperature control loop in CS2 can effectively handle the disturbance to product purity compared to CS1.

When 5% step feed change of acetonitrile composition introduced, the performances of streams are similar to those in the basic control structure CS1, as shown in Fig. 16(a). Moreover, in Fig. 16(b), ERC temperature (T2) keeps a stable value with a very small overshoot of 2°C and has a transient settling out time of 0.5 h. As to products, the purity of *n*-propanol (X_{D2}) changes smoothly and reaches to the desired purity with no deviations. In conclusion, the CS2 has better dynamic responses than CS1.

Conclusion

Design and control of an extractive distillation for separation of acetonitrile and *n*-propanol are proposed in this paper. NMP is selected as a suitable entrianer via a selection criterion. Using the minimum energy consumption as the objective function, the optimal design of the extractive distillation process is presented with the multiparameter optimization analysis.

The two control structures are performed for the distillation process. Feed flow rate and composition disturbances are introduced to verify their response. The control structure CS1 with a temperature–composition cascade control loop shows quite good performance only on the EDC. To get a more robust control, the improved control structure CS2 with an average temperature control loop is adopted. The dynamic results demonstrate that CS2 can stabilize the temperature fluctuation and maintain high purity of two

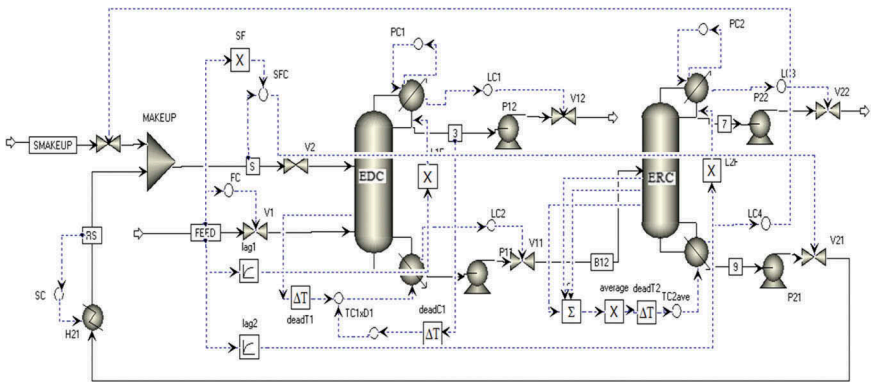

Figure 14. Diagram of control structure CS2.

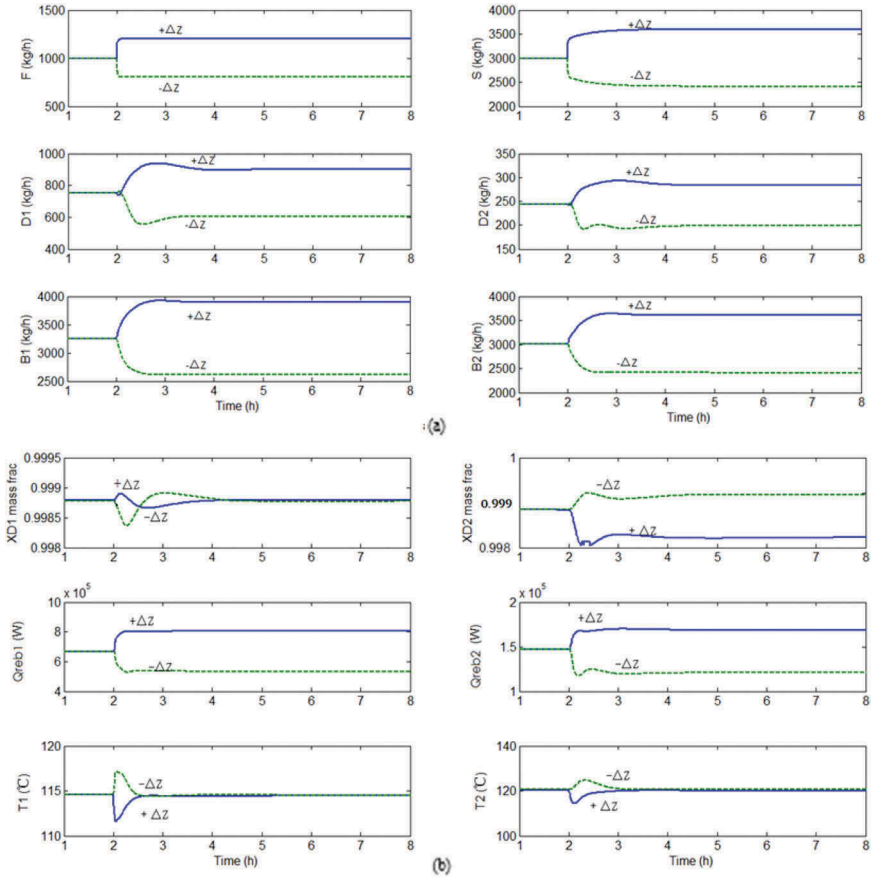

Figure 15. CS2 dynamic response curve of variables in feed flow ±20% disturbance.

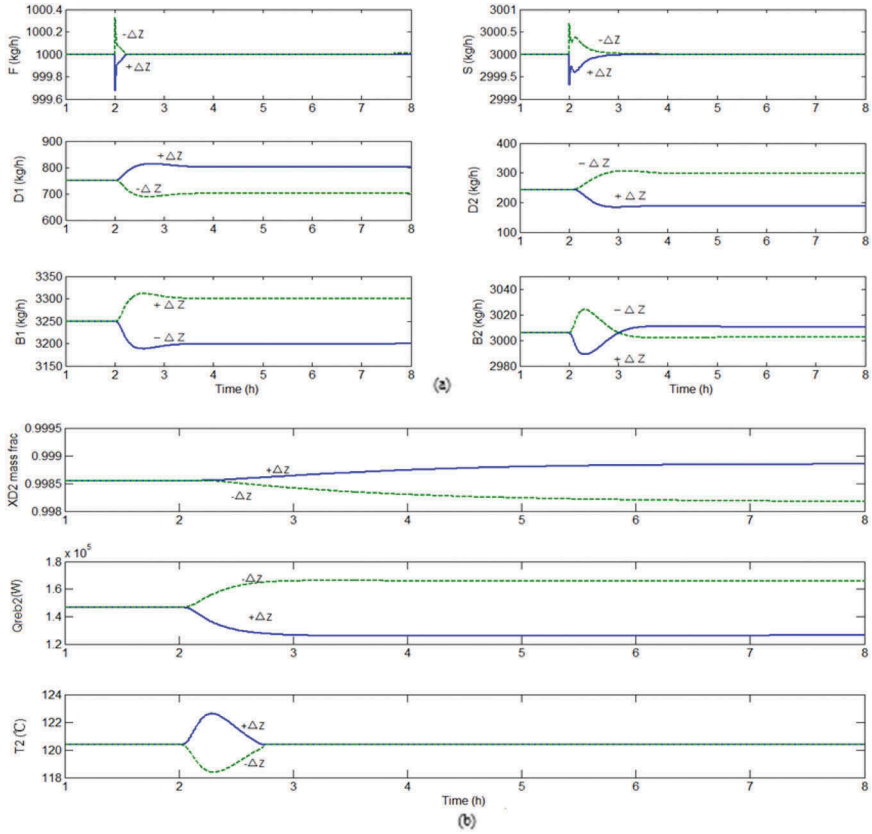

Figure 16. CS2 dynamic response curve for the feed composition of acetonitrile ±5%.

products effectively. Consequently, CS2 is recommended for this extractive distillation process.

List of symbols

DMF	dimethylformamide
DMSO	dimethyl sulfoxide
NMP	*N*-methyl pyrrolidone
RCM	residue curve map
EDC	extractive distillation column
ERC	entrainer recovery column
F	feed flow rate [kg/h]
N_1, N_2	stage number of EDC and ERC
N_{F1} and N_{F2}	feed position of EDC and ERC
N_S	solvent feed position
D1, D2	distillate rate of EDC and ERC [kg/h]
B1, B2	bottom rate of EDC and ERC [kg/h]
R1, R2	reflux ratio of EDC and ERC
X_{D1}, X_{D2}	mass fraction of products in distillate
T_b	bubble points [°C]
T_{F1}	feed temperature [°C]
T_S	solvent feed temperature [°C]
Q_{reb1} and Q_{reb2}	reboiler duty of EDC and ERC [kW]
Q_{con1} and Q_{con2}	condenser duty of EDC and ERC [kW]
K_c	steady-state gain
τ	integral time [min]

References

[1] Yi, W.; Zhiwu, W.; JingKai, G.; Yingwu, W. (2008) Determination of acetonitrile volume fraction in mobile phase by HPLC. *Chemical Research in Chinese Universities*, 24: 694–696.

[2] Zhian, Z.; Yanqing, L.; Jie, L.; Yexiang, L. (2009) Electrochemical behavior of wound supercapacitors with propylene carbonate and acetonitrile based non-aqueous electrolytes. *Journal of Central South University*, 16: 247–252.

[3] Xiaohong, W.; Li, X.; Peng, T.; Guangzhen, T. (2016) Design and control of extractive dividing wall column and pressure-swing distillation for separating azeotropic mixture of acetonitrile/N-propanol. *Chemical Engineering and Processing*, 110: 172–187.

[4] Luo, H.; Bildea, C.S.; Kiss, A.A. (2015) Novel heat-pump-assisted extractive distillation for bioethanol purification. *Industrial & Engineering Chemistry Research*, 54: 2208–2213.

[5] Anokhina, E.; Timoshenko, A. (2015) Criterion of the energy effectiveness of extractive distillation in the partially thermally coupled columns. *Chemical Engineering Research & Design*, 99: 165–175.

[6] Luyben, W.L.;. (2008) Comparison of extractive distillation and pressure-swing distillation for acetone/chloroform separation. *Computers & Chemical Engineering*, 50: 1–7.

[7] Knapp, J.P.; Doherty, M.F. (1992) A new pressure-swing-distillation process for separating homogeneous azeotropic mixtures. *Industrial & Engineering Chemistry Research*, 31: 346–357.

[8] YuPing, H.; Anyuan, J. (2005) Seperation of acetonitrile and propyl alcohol using extractive distillation with salt. *Journal of Shaoyang University*, 2: 109–110.

[9] Jing, F.; Jing, L.; Chunli, L.; Yang, L. (2013) Isobaric vapor-liquid equilibrium for the acetonitrile water system containing different ionic liquids at atmospheric pressure. *Journal of Chemical & Engineering Data*, 58: 1483–1489.

[10] Hanxue, Z.; Peng, B.; Ruichang, G. (2014) Separation of acetonitrile-1-propanol by extractive distillation. *Chemical Industry and Engineering*, 31: 35–40.

[11] Lohmann, J.; Joh, R.; Nienhaus, B.; Gmehling, J. (2015) Revision and extension of the group contribution method modified UNIFAC. *Chemical Engineering & Technology*, 21: 245–248.

[12] Yao, J.Y.; Lin, S.Y.; Chien, I.L. (2007) Operation and control of batch extractive distillation for the separation of mixtures with minimum-boiling azeotrope. *Journal of the Chinese Institute of Chemical Engineers*, 38: 371–383.

[13] Yuan, S.; Zou, C.; Hong, Y.; Chen, Z.; Yang, W. (2015) Study on the separation of binary azeotropic mixtures by continuous extractive distillation. *Chemical Engineering Research & Design*, 93: 113–119.

[14] Luyben, W.L.; Chien, I.L. (2010) *Design and Control of Distillation Systems for Separating Azeotropes*, John Wiley & Sons: Hoboken, NJ.

[15] Milani, S.M.;. (1999) Optimization of solvent feed rate for maximum recovery of high purity top product in batch extractive distillation. *Chemical Engineering Research & Design*, 77: 469–470.

[16] Honghai, W.; Xiaoying, C.; Hongwei, Z.; Chunli, L. (2011) Optimization of operating parameters for a complex column combined with response surface methodology and process simulation. *Chinese Journal of Hebei University*, 40: 30–40.

[17] Luyben, W.L.;. (2008) Effect of solvent on controllability in extractive distillation. *Industrial & Engineering Chemistry Research*, 47: 4425–4439.

[18] Luyben, W.L.;. (2013) *Distillation Design and Control Using Aspen Simulation*, John Wiley & Sons: Hoboken, NJ.

[19] And, F.R.; Luyben, W.L. (2000) Extensions of the simultaneous design of gas-phase adiabatic tubular reactor systems with gas recycle. *Industrial & Engineering Chemistry Research*, 40: 635–647.

[20] Shengkai, Y.; Yujie, W.; Guangyue, B.; Yong, Z. (2013) Design and control of an extractive distillation system for benzene/acetonitrile separation using dimethyl sulfoxide as an entrainer. *Industrial & Engineering Chemistry Research*, 52: 13102–13112.

[21] Gil, I.D.; Gómez, J.M.; Rodríguez, G. (2012) Control of an extractive distillation process to dehydrate ethanol using glycerol as entrainer. *Computers & Chemical Engineering*, 39: 129–142.

[22] Rafiqul, G.; Jose, A.R.; George, S. (1986) Control studies in an extractive distillation process simulation and

measurement structure. *Chemical Engineering Communications*, 40: 281–302.

[23] Hsu, K.Y.; Hsiao, Y.C.; Chien, I.L. (2016) Design and control of dimethyl carbonate-methanol separation via extractive distillation in the dimethyl carbonate reactive-distillation process. *Industrial & Engineering Chemistry Research*, 49: 735–749.

[24] Saiful, A.; Chien, I.L. (2007) Combined preconcentrator/recovery column design for isopropyl alcohol dehydration process. *Industrial & Engineering Chemistry Research*, 46: 2535–2543.

[25] Zhenyu, B.; Weijiang, Z.; Xianbao, C.; Xu, J. (2014) Design, optimization and control of extractive distillation for the separation of trimethyl borate–methanol. *Industrial & Engineering Chemistry Research*, 53: 14802–14814.

[26] Gani, R.; Brignole, E.A. (1983) Molecular design of solvents for liquid extraction based on UNIFAC. *Fluid Phase Equilibria*, 13: 331–340.